PROBABILISTIC ASSESSMENT OF PERMANENT GROUND DISPLACEMENT ACROSS EARTHQUAKE FAULTS

Maria I. Todorovska,[1] Mihailo D. Trifunac[2] and Vincent W. Lee[3]

[1,2]*University of Southern California, Dept. of Civil and Envir. Eng., KAP 210, Los Angeles, CA, U.S.A.*
[1]*E-mail: mtodorov@usc.edu;* [2]*E-mail: trifunac@usc.edu;* [2]*E-mail: vincent.w.lee@usc.edu*

ABSTRACT

A methodology is presented for the assessment of permanent ground displacement across a fault, due to a slip on that fault caused by an earthquake. Such estimates are important for the design and retrofit of highway bridges and tunnels crossing faults, as well as for other lifelines crossing faults, such as aqueducts, water and gas lines, etc. The methodology is developed within the framework of probabilistic seismic hazard analysis. The earthquake occurrences are modeled as Poisonian sequences. Besides the earthquake occurrence rates, this model requires probabilities that the rupture affects the site (i.e. breaks the surface and extends to the site), and probability distribution function of the displacement at the surface, given that the earthquake has ruptured the surface. For the latter, a scaling law is used that is consistent with scaling laws for peaks and spectra of strong ground shaking, developed earlier by the authors for Western U.S. Results are presented for two hypothetical faults.

Keywords: Probabilistic seismic hazard assessment, fault displacement hazard, lifelines.

1. INTRODUCTION

In densely populated areas near the continental margins, characterized by numerous faults with moderate to high seismic activity, lifelines (highway bridges and tunnels, aqueducts, gas lines) crossing active faults are not uncommon (e.g. Vincent Thomas Bridge in the Los Angeles area, crossing the Palos Verdes Fault; San Diego–Coronado Bay Bridge, crossing strands of the Rose Canyon Fault Zone; Bart Tunnel in Berkeley Hill and Clermont Water Tunnel in northern California, crossing the Hayward Fault; Devils Slide Tunnel in the San Francisco Bay area, which is an area of high seismic activity comprising of the San Andreas Fault and San Gregorio Fault). For the design and retrofit of such structures, and for the assessment of their seismic performance, it is valuable to have

rational estimates of the permanent ground displacement caused by seismic slip. This paper presents a *probabilistic* methodology for the assessment of permanent ground displacement across a fault, due to slip on that fault caused by an earthquake. Results are presented for two hypothetical strike-slip faults, with characteristics similar to Class A and B faults in California, where Class A are the most active faults, with average slip rate grater than 5 mm/year, and Class B are all other faults (Cao et al., 2003).

The probabilistic framework makes it possible to compare not only multiple risks to a structure caused by earthquakes, but also to compare the seismic risk with risks from other natural and man made hazards, and with other voluntary or involuntary risks to individuals and society. In comparing risks to a structure from different consequences of earthquakes, it is important that the respective methodologies are *compatible*. The presented model is *compatible with hazard models for strong ground shaking and its consequences in California*, e.g. peak acceleration, response spectrum amplitudes, peak ground strain, and soil liquefaction developed earlier by the authors of this report and co-workers (Lee and Trifunac, 1987; Trifunac, 1991; Todorovska and Trifunac, 1996, 1999). It differs from the model of Youngs et al. (2003), which is for *normal* faulting environment, aimed at application to the potential Yucca Mountain nuclear waste repository site in Nevada, in that is uses scaling laws specific for faults in California, which is in a shallow seismogenic zone, with predominantly *strike-slip* mechanism of faulting. Another important difference is that it is *compatible* with scaling laws for prediction of ground shaking hazard (peak amplitudes, spectra, peak ground strain, and occurrence of soil liquefaction), while Youngs et al. (2003) use scaling laws that were developed using only fault dislocation data.

2 METHODOLOGY

The probabilistic hazard methodology for fault displacement hazard differs from the one for ground shaking hazard (and related consequences, e.g. soil liquefaction) in that it involves only one source zone, and that not every earthquake in that source zone affects the site (while every earthquake would cause some level of shaking, depending on the distance). Part (a) of Fig. 1 shows a fault with length L and width W, dipping at angle δ, and extending from the ground surface to depth $H = W \sin\delta$. Part (b) shows the fault surface, the site, and three possible ruptures, one of which affects the site, another one that occurs at depth and does not break the ground surface, and a third one that breaks the ground surface but does not extend horizontally to the site. The possible ruptures have lengths $L_R(M)$ and widths $W_R(M)$, which both depend on magnitude. Simplifying assumptions in the model are that the displacement at the ground surface is uniform and continuous along the ruptured segment of the fault trace, and that the static displacement field does not decreases much with distance from the fault, which is appropriate for typical bridges, which have spans of the order of hundred meters, in which case this "attenuation" effect is small compared to the overall uncertainty of the estimation.

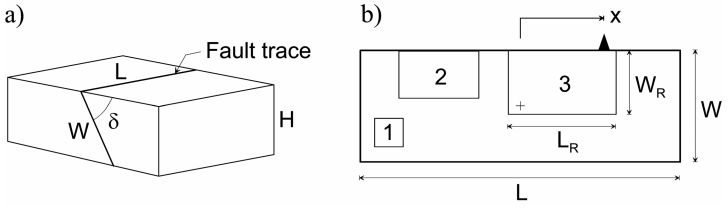

Fig. 1 The model.

Let D be a random variable representing, for an earthquake that has ruptured the ground surface, the absolute value of the displacement across the rupture at the ground surface, and D_{site} be the same type of displacement *at the site*, which may or may not have been affected by the earthquake, and let $p(d,t)$ be the probability that D_{site} exceeds level d during exposure period t. We assume that the earthquakes occur as a Poissonian sequence in time (i.e. independently of one another, at a constant rate depending on magnitude), and discretize the earthquake magnitudes (for events with time dependent rate, see Todorovska et al. 2005). Let $M_i, i = 1,...,N_i$ be the possible discrete magnitudes, and $n_i(t)$ be the corresponding expected number of earthquakes during exposure t. Then, the expected number of exceedances of level d during exposure period t is

$$m(d,t) = \sum_{i=1}^{L} q_i(d) n_i(t) \tag{1}$$

where $q_i(d)$ is the conditional probability

$$q_i(d) = P\left\{D_{\text{site}} > d \,\middle|\, \text{event } M = M_i \text{ occurred}\right\} \tag{2}$$

Then the probability of exceeding level d is

$$p(d,t) = P\left\{D_{\text{site}} > d \,\middle|\, t\right\} = 1 - e^{-m(d,t)} \tag{3}$$

The conditional probability $q_i(d)$ can be expressed as the product of three probabilities

$$q_i(d) = P\left\{D > d \,\middle|\, \text{event } M = M_l \text{ occurred}\right\} P\left\{\begin{matrix}\text{rupture breaks}\\ \text{ground surface}\end{matrix}\right\} P\left\{\begin{matrix}\text{rupture extends}\\ \text{horizontally to the site}\end{matrix}\right\} \tag{4}$$

The likelihood that a rupture will break the ground surface can be estimated specifically for a fault based on: direct observations during prior earthquakes, the hypocentral depth distribution during past earthquakes, relations for rupture width versus earthquake magnitude, etc. For the purpose of demonstrating the methodology, in this paper we assume that thise likelihood is larger for larger magnitude earthquakes, which have larger rupture width, $W_R(M)$, compared to the width of the fault, W, and we adopt

$$P\left\{\begin{matrix}\text{rupture breaks}\\ \text{ground surface}\end{matrix}\right\} = \min\left(1, \frac{W_R(M)}{W}\right) \equiv r_W\left(W, W_R\right) \tag{5}$$

Similarly, we assume that the likelihood that the ruptured segment of the fault, $L_R(M)$, would extend to the site would be larger for larger magnitude earthquakes, which have larger rupture length, but would also depend on where the site is located relative to the edges of the fault (due to the constraint that the rupture has to fit along the fault length, L). For equal likelihood that a rupture will occur anywhere along the length of the fault, as long as it fits within the fault length

$$P\left\{\begin{array}{l}\text{rupture}\\ \text{extends}\\ \text{horizontally}\\ \text{to the site}\end{array}\right\} = \begin{cases} 1, & L_R(M) \geq L \\ \min\left(1, \dfrac{L_R(M)}{L - L_R(M)}\right), & L_R(M) < L, \quad |x| \leq \dfrac{L}{2} - L_R(M) \equiv r_L(L, L_R, x) \\ \min\left(1, \dfrac{(L/2) - |x|}{L - L_R(M)}\right), & L_R(M) < L, \quad |x| > \dfrac{L}{2} - L_R(M) \end{cases} \tag{6}$$

where $|x|$ is the distance of the site from the center of the fault (see Fig. 1).

For estimating probabilities r_W and r_L, we initially considered using the relations for L_R and W_R of Trifunac (1993a,b), and of Wells and Coppersmith (1994), but opted for our own relations

$$\log_{10} L_R(M) = 0.5113\, M - 1.9341; \qquad \log_{10} W_R(M) = 0.2292\, M - 0.5128 \tag{7}$$

which we derived by least squares fit through a subset of the data gathered by Wells and Coppersmith (1994) that corresponds to California earthquakes. Fig. 2 shows L_R and W_R versus magnitude for model 3 of Trifunac (1993a,b) (the medium thick lines), consistent with *seismological* estimates of rupture length and width, with theoretical earthquake source models, and with empirical scaling models of peaks and spectra of strong ground motion (Lee et al., 1995; Trifunac, 1993a). Fig. 2 also shows empirical relations for L_R and W_R of Wells and Coppersmith (1994) (the thin lines) for "all" types of faulting, derived from worldwide

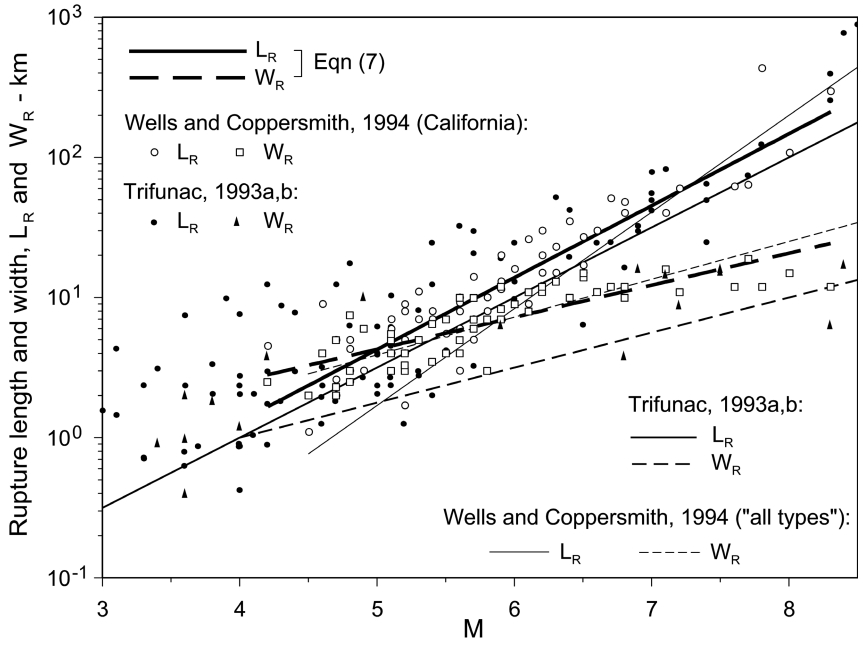

Fig. 2 Rupture length and width.

data, and valid for $4.8 \le M \le 7.9$. The open circles and rectangles show a subset of the data for L_R and W_R gathered by Wells and Coppersmith (1994) for earthquakes in California. The corresponding full symbols show data gathered by Trifunac (1993a,b) from various published seismological estimates. The thick lines represent L_R and W_R as defined in eqn (7) and used in this paper.

The most delicate part of the hazard model is the choice of scaling law for the permanent displacement across the fault. We considered adopting one of the published models, in particular, those of Wells and Coppersmith (1994), and the models for $d_{\max}$ of Lee et al. (1995). The former present models that are linear fits through worldwide data for the logarithm of surface displacement versus earthquake magnitude, separately for different types of faulting, and also for all types of faulting, valid within the range of the data. For example, for the case of "all" types of faulting (for which the regression is most stable due to the largest number of data points) they use data from 148 events, and their model is valid for magnitudes between 5.6 and 8.1. The standard deviation of the logarithm of the displacement for this regression is 0.36, or a factor of 2.3, which is comparable to the scatter of the scaling laws for prediction of amplitudes of ground shaking. The models for $d_{\max}$ of Lee et al. (1995) predict peak ground displacement as a function of earthquake magnitude, distance from the source, propagation type characteristics, and various combinations of geologic site and local soil conditions. Their models were derived by multi-step regression analysis of strong motion data of peak ground displacement (computed from recorded accelerograms, after correction for the reduction due to baseline correction and high-pass filtering) from about 2,000 three-component accelergrams recorded in the Western U.S., in such a way that *on the fault* (at zero epicentral distance) they are consistent with fault dislocation data. Based on extrapolations using physical source models, their models are valid for all magnitudes, and predict decay with distance near the source consistent with a theoretical model of radiation from a dislocation. Further, these models are also consistent with the long period asymptote of the frequency dependent attenuation models of Lee and Trifunac (1995a,b) of ground motion in the near field. The scatter of their model is such that the standard deviation of $\log_{10} d_{\max}$ is 0.38, or a factor of 2.4. We opted for one of the models of Lee et al. (1995) because of their consistency with ground shaking hazard models, which is important for structures sensitive both to ground shaking and to static displacements. As the uncertainty in the

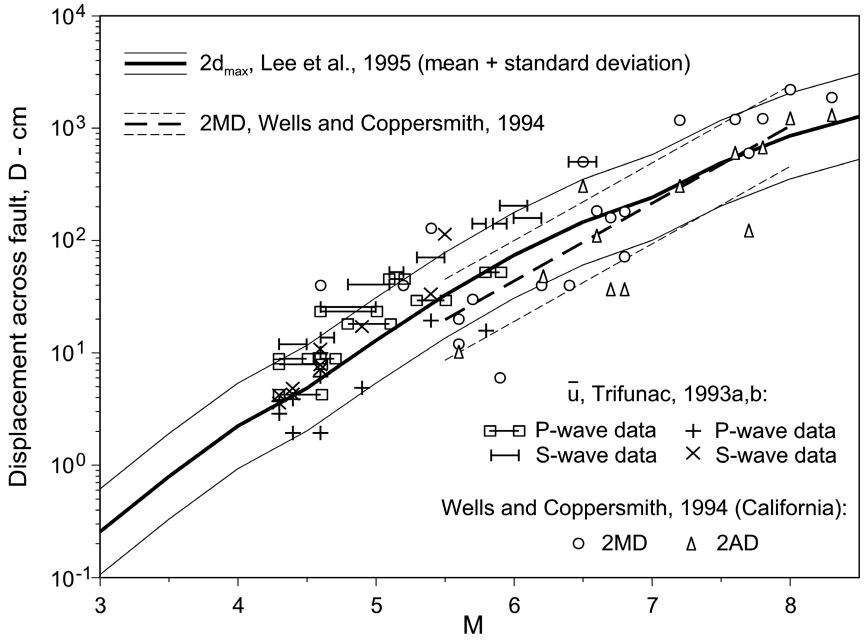

Fig. 3 Data and scaling laws for D for earthquakes in California.

predictions remains relatively large (grater than a factor of 2), for meaningful comparison and weighting of different hazards and their consequences upon a structure, it is essential that the scaling laws are consistent.

We assume symmetric rupture, in which case the displacement at the ground surface across the fault, $D=2d_{\max}$. While the displacement along the trace of the fault varies, and may even be discontinuous, we assume that the scaling law predicts the *average* over the length of the rupture, and that the variability is captured by the scatter of the scaling law for $d_{\max}$. In particular, we adopted the Mag + site + soil + % rock path model for $d_{\max}$ of Lee et al. (1995), at epicentral distance $R = 0$, hypocentral depth $H_R = 0.5\, W_R \sin\delta$ (see Fig. 1), and for the following path and site conditions: $r = 1$ (entire travel path is through rock), $s = 2$ ("rock" geologic site condition) and $s_L = 0$ ("rock" local soil condition). Lee et al. (1995) also analyzed the distribution of the residuals of $\log_{10} d_{\max}$, and showed that normal distribution with mean -0.0090 and the standard deviation 0.3975 is reasonably close to the actual one. Hence, D is modeled as lognormal random variable, such that $\log_{10} D$ has mean

$$\begin{aligned}\mu = {} & M - 2.2470\log_{10}\left[\Delta\left(M, R=0, H_R = 0.5\, W_R \sin\delta, S, S_0\right)/L_R\right] + 0.6489M \\ & +0.0518*2 - 0.3407v - 2.9850 - 0.1369M^2 - 0.0306 + \log_{10} 2 - 0.0090\end{aligned} \tag{8}$$

and standard deviation $\sigma = 0.3975$, where D is in cm, M—earthquake magnitude, Δ—(in km) "representative" source to station distance. The "representative" source to station distance, first proposed by Gusev (1983), depends both on physical distance and on the size of the rupture

$$\Delta = S\left(\ln\frac{R^2 + H_R{}^2 + S^2}{R^2 + H_R{}^2 + S_0^2}\right)^{-1/2} \tag{9}$$

where S—source dimension, and S_0—source coherence radius (both functions of magnitude), and is never zero, even for a point on the fault.

Fig. 3 shows $D=2d_{\max}$ versus magnitude, as predicted by the model (the thick lines), against the data for average dislocation, $\bar{u}$, gathered by Trifunac (1993a,b), and the data for average (AD) and maximum (MD) displacement gathered by Wells and Coppersmith (1994) for California earthquakes. It can be seen that the model is in good agreement with the data. This figure also shows the regression model of Wells and Coppermith (the weaker lines) for average displacement for "all" types of faulting.

3 RESULTS AND ANALYSIS

The model is illustrated by results for two hypothetical vertical strike-slip faults. Fault I represents a Class B, and fault II—a Class A fault in California, where Class A are those faults with average slip rate $\dot{\bar{u}} > 5$ mm/year, and Class B are all other faults (Cao et al., 2003). In the 2002 revision of the national seismic hazard maps (Frankel et al., 2002; Cao et al., 2003), for the Class A faults, 100% of

the seismic moment is assigned to characteristic events, while for Class B faults, 2/3 of the moment is assigned to characteristic events and 1/3 — to Gutenberg-Richter events, with b = 0.8. The seismic moment rate $\dot{M}_0$ and the average slip rate $\dot{\bar{u}}$ are related by $\dot{M}_0 = \mu A \dot{\bar{u}}$ where A is the area of the fault and $\mu \sim 3*10^{11}$ dyne/cm^2 is the shear modulus for the region (Working Group on California Earthquake Probabilities, 2003). For our hypothetical Class B fault, we follow the 2/3 and 1/3 partitioning of seismic moment, while, for the hypothetical Class A fault, we consider three variants—one of which is partitioning as for Class B faults, and the other two are 100% assigned to characteristic events—and examine their effect on the final result. For both faults, the magnitude of the characteristics events is distributed near the maximum magnitude for the fault, with average occurrence rates over this range decreasing with magnitude according to a Gutenberg-Richter law with b = 0.5. The properties of the hypothetical faults I and II are summarized in Table 1. In the results that follow, for hypothetical fault I, we compare the contributions to the hazard from the two earthquake populations at a site at the center of the fault, and we compare the hazard at sites that are at different locations along the fault. Similarly, for fault II, we compare the hazard for the three variants of distribution of seismic moment. Results are shown for the expected number of exceedances in 50 years, and the probability of exceedance, all versus different levels of displacement across the fault, d. The range of d is from as small as 1 mm to as large as 100 m, to examine the asymptotic trends.

Table 1 Parameters for Hypothetical Faults I and II

Hypothetical Faults I (Class B)	
L = 100 km, H = 13 km, δ = 90°	
G-R:	Characteristic:
$\dot{M}_0 = 38\times10^{22}$ dyn × cm/yr b = 0.8, M_{max} = 7.5	$\dot{M}_0 = 75\times10^{22}$ dyn × cm/yr b = 0.5, 6.5 < M < 7.5

Hypothetical Faults II (Class A)		
L = 100 km, H = 18 km, δ = 90°		
IIa	G-R:	Characteristic:
	$\dot{M}_0 = 4.45\times10^{24}$ dyn × cm/yr b = 0.8, M_{max} = 7.5	$\dot{M}_0 = 8.9\times10^{24}$ dyn × cm/yr b = 0.5, 6.75 < M < 7.75
IIb	G-R:	Characteristic:
		$\dot{M}_0 = 13.35\times10^{24}$ dyn × cm/yr b = 0.5, 6.75 < M < 7.75
IIc	G-R:	Characteristic:
		$\dot{M}_0 = 13.35\times10^{24}$ dyn × cm/yr b = 0.5, 7.25 < M < 7.75

Figure 4 shows results for hypothetical fault I. Part (a) shows the distribution of the expected number of earthquakes in 50 years, and part (b) shows the probabilities r_W and r_L that the rupture will break the surface and will extend horizontally to the site for x = 0, 10, 25, 40 and 49 km. The trend seen from part (b) is that, in general, the probability of being affected by a rupture grows with magnitude, and is larger for sites closer to the center of the fault (x = 0). However, for sufficiently small magnitudes (how small it depends on x), this probability does not depend on the location of the site, as only a fraction of such earthquakes could affect any site on the fault. For larger magnitudes, this probability becomes larger for a site at the center. For very large magnitudes, as the rupture length approaches L, all sites on the fault would be affected, i.e. $r_L(M) \to 1$ for all x. However, as a result of discretization of the magnitude, the largest discrete magnitude is smaller than M_{max}, which results in $r_L(M)$<1 for

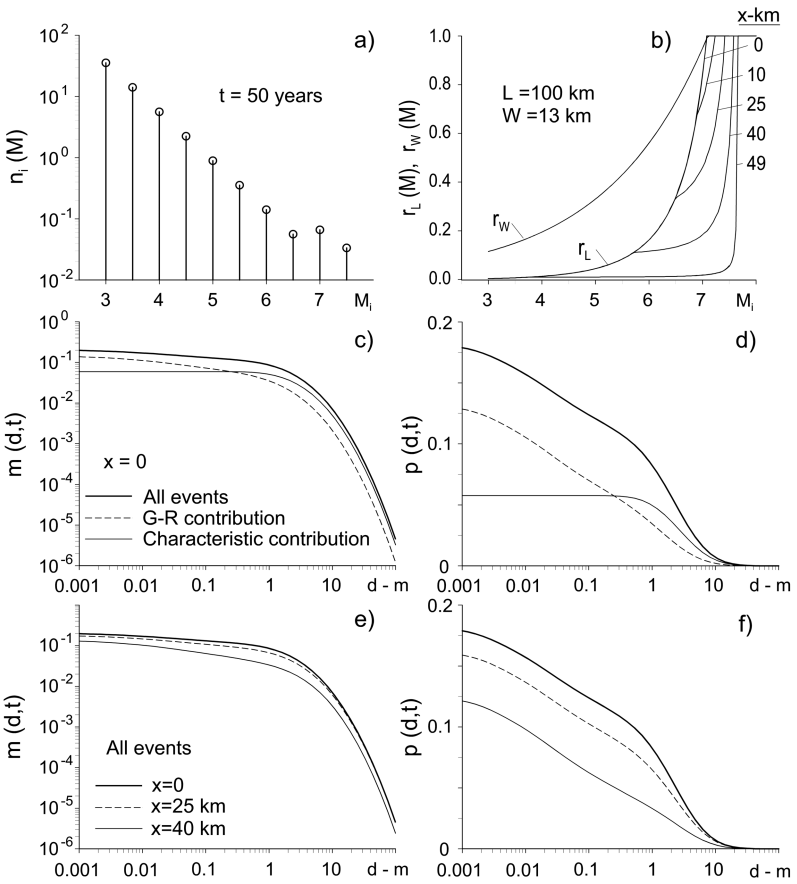

Fig. 4 Results for Hypothetical fault I (Class B).

sites sufficiently far from the center. Parts (c) and (d) compare the contributions to the hazard from all events with that only from the Gutenberg-Richter and only from the characteristic events, for a site at the center of the fault ($x = 0$). As it can be expected, the hazard is smaller for larger levels of *d*, and it rapidly decreases with *d* for values grater than several meters. For significant level of *d* (larger than several cm), the contribution from the characteristic events (i.e. larger magnitude events) is larger than the one from the Gutenberg-Richter events. As a result of the small seismicity and the fact that not every earthquake affects the site, the hazard is generally small. For example, for d = 50 cm, the probability of exceedance in 50 years is about 0.1. Parts (e) and (f) compare the hazard for sites at different distances from the center of the fault, at x = 0, 25 and 40 km. It can be seen that the hazard is the largest for the site at the center, and is slightly smaller for the site at 1/4 fault length distance from the edge (x = 25 km). The difference between the hazard at these three sites decreases with increasing *d* for which the hazard is very small everywhere along the fault. For d = 50 cm, the probability of exceedance drops from 0.1 at x = 0 to less than half of that value at x = 40 km.

Figure 5 shows similarly results for hypothetical fault II. Results are compared for the three variants of distribution of seismic moment, IIa, IIb and IIc (see Table 1), for a site at the center of the fault ($x = 0$). We recall that for models IIb and IIc, all earthquakes are characteristic. It can be seen from part (a) that, due to the specific discretization scheme, the characteristic earthquakes for variants IIa and IIb have magnitude M = 7 and 7.5, while for variant IIc, they have only magnitude M = 7.5, and their number is small, despite the fact that all of the seismic moment is assigned to characteristic events, because of the very large moment release for large magnitudes, which grows exponentially with magnitude. It can be seen from part (c) and (d) that the hazard is the largest for variant IIa, for which 1/3 of the seismic moment is assigned to Gutenberg-Richter events, and is the smallest for variant IIc, for which the characteristic events, to which all the moment is assigned to, are distributed over a shorter magnitude interval near the maximum magnitude (Table 1). This can be explained by the significantly smaller expected number of events, which is not compensated for sufficiently by their stronger effects, except for the very high levels of displacement, for which the results of all three

models become the same. It can also be seen that the results for d less than several tens of centimeters, the hazard for variants IIb and IIc does not grow with decreasing d. For small d, the probability of exceedance approaches 0.2 for variant IIc, and 0.38 for variant IIb, while it continues to grow with decreasing d for variant IIa.

To compare some numbers, for d = 50 cm, p = 0.44 for variant IIa, p = 0.37 for variant IIb, and p = 0.2 for variant IIa, while p = 0.1 for fault I, which has an *order of magnitude* smaller seismic moment rate. For d = 1 m, p = 0.38 for variant IIa, p = 0.34 for variant IIb, and p = 0.19 for variant IIa, while p = 0.08 for fault I. For a large displacement, e.g. d = 10 m, $p \approx 0.04$ for all variants for fault II, and is insignificant for fault I.

4 CONCLUSIONS

It can be concluded that (1) the fault displacement hazard is in general small, due to the fact that only one fault contributes to the hazard and not every event on that fault affects the site. For the illustrations in this paper, for 50 years exposure, the probability that D > 1 cm is about 0.18 for the hypothetical Class B fault, and abut 0.6, 0.38 and 0.2 for the three variants of distribution of seismic moment for the hypothetical Class A fault.

(2) The results are quite sensitive to how the seismic moment is distributed over earthquake magnitudes, which is mostly based on the judgment of the hazard modeler, or is a result of consensus building (implemented by logic trees; Working Group on California earthquake probabilities, 2003), due to insufficient data to determine this more uniquely, and changes with time as more information on the faults becomes available. The trend is that distribution of seismic moment over larger magnitudes may lead to significantly smaller estimates of the hazard (e.g., a factor of two or more for the probability of exceedance of one or several meters of displacement across fault II).

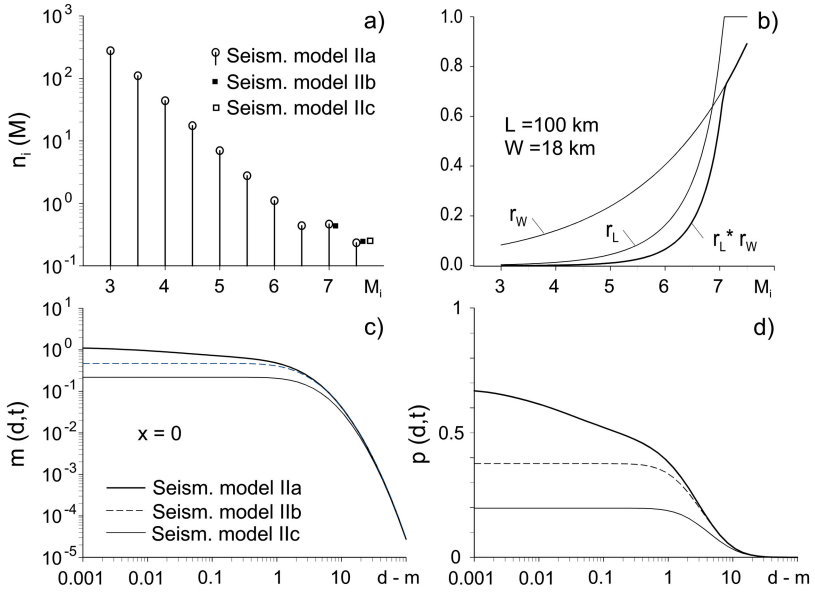

Fig. 5 Results for Hypothetical fault II (Class A).

(3) The hazard is the largest near the center of the fault and decreases towards the edges. This effect results from a hypothetical but physically plausible estimate of the probability that a rupture would extend horizontally to

the site, $r_L(M)$, based on the assumption of uniform probability of the rupture occurring anywhere along the fault length as long as it fits within the fault length. The consequences of nonuniform rupture probability along the fault length can be evaluated based on prescribed hypotheses, a priori (e.g. consideration of seismic gaps), by modifying r_W and r_L in eqns (13) and (14). We will describe how this is done in future papers. Hence, for the examples illustrated in this paper, the dependence of the hazard on the location of the site along the fault is purely geometric, and depends on the rupture length, which is a function of earthquake magnitude, and on the length of the fault.

The model in this paper assumes that, for a rupture that breaks the surface, the dislocation at the surface is uniform along the entire rupture length. In reality, the dislocation at the surface is nonuniform and may be discontinuous, but the general tendency is that it decreases towards the edges of the rupture (Wells and Coppersmith, 1994; Youngs et al., 2003). Further, a comparison of the adopted model for *D* with independent data from Wells and Coppersmith (1994) for average (AD) and maximum (MD) surface displacement (for California faults) shows that our model is more consistent with the data for maximum displacement (see Fig. 3).

For application to a specific fault, it is recommended that, to the extent possible, fault specific (or region specific) information be used to define the probabilities that a rupture will break the ground surface (e.g. based on the distribution of hypocenters) and would extend horizontally to the site, and that most current seismicity information is used. An interesting problem to be addressed by future research is to compare the hazard for permanent displacement across a fault due to dislocation on the fault with the hazard for dynamic differential motion, and where applicable—with the hazard for differential motion due to consequences of soil liquefaction and lateral spreading.

ACKNOWLEDGEMENTS

This work was supported by a grant from METRANS—a U.S. Department of Transportation (DOT) designated University Transportation Center (Grant No. 03-27). The authors are grateful to Anoosh Shamsabadi from Caltrans for the many useful discussions on the application aspect of this project.

REFERENCES

1. Cao T., Bryant W.A., Rowshandel B., Branum D., Wills C.J. (2003). The revised 2002 California probabilistic seismic hazard maps, www.consrv.ca.gov/CGS/rghm/psha/.

2. Frankel, A.D., Petersen M.D., Mueller C.S., Haller K.M., Wheeler R.L., Leyendecker E.V., Wesson R.L., Harmsen S.C., Cramer C.H., Perkins D.M., Rukstales K.S. (2002). Documentation for the 2002 Update of the National Seismic Hazard Maps, Open File Report 03-420, U.S. Geological Survey, U.S. Department of the Interior, Denver, Colorado.

3. Gusev A.A. (1983). Descriptive statistical model of earthquake source radiation and its application to an estimation of short-period strong motion, *Geophys. J. Royal Astr. Soc.* **74:3**, 787–808.

4. Lee V.W., Trifunac M.D. (1987). Microzonation of a metropolitan area, Dept. of Civil Eng. Report No. CE 82-02, Univ. of Southern California, Los Angeles, California.

5. Lee V.W., Trifunac M.D. (1995a). Frequency dependent attenuation function and Fourier amplitude spectra of strong earthquake ground motion in California, Dept. of Civil Engineering Report No CE 95-03, University of Southern California, Los Angeles, California.

6. Lee V.W., Trifunac M.D. (1995b). Pseudo Relative Velocity Spectra of Strong Earthquake Ground Motion in California, Dept. of Civil Engineering Report No CE 95-04, University of Southern California, Los Angeles, California.

7. Lee V.W., Trifunac M.D., Todorovska M.I., Novikova E.I. (1995). Empirical equations describing attenuation of the peaks of strong ground motion, in terms of magnitude, distance, path effects and site conditions, Dept. Civil Eng. Report No. 95-02, Univ. Southern California, Los Angeles, California.

8. Todorovska M.I., Trifunac M.D. (1996). Hazard mapping of normalized peak strain in soil during earthquakes: microzonation of a metropolitan area, *Soil Dynam. and Earthqu. Eng*. **15:5**, 321-329.

9. Todorovska, M.I., Trifunac M.D. (1999). Liquefaction opportunity mapping via seismic wave energy, *J. Geotech. and Geoenv. Eng*., ASCE **125:12**, 1032-1042.

10. Todorovska M.I., Trifunac M.D., Lee V.W. (2005). Shaking hazard compatible methodology for probabilistic assessment of permanent ground displacement across earthquake faults, *Soil Dynam. and Earthqu. Eng*., submitted for publication.

11. Trifunac M.D. (1991). A Microzonation method based on uniform risk spectra, *Soil Dynam. & Earthqu. Engng* **9:1**, 34–43.

12. Trifunac M.D. (1993a). Broad Band Extension of Fourier Amplitude Spectra of Strong Motion Acceleration, Dept. of Civil Eng., Rep. No. CE 93-01, Univ. Southern California, Los Angeles, California.

13. Trifunac M.D. (1993b). Long period Fourier amplitude spectra of strong motion acceleration, *Soil Dynam. & Earthqu. Engng* **12:6**, 363–382.

14. Wells D.L., Coppersmith K.J. (1994). New empirical relationships among magnitude, rupture length, rupture width, rupture area, and surface displacement, *Bull. Sesm. Soc. Am*. **84:4**, 974-1002.

15. Working Group on California Earthquake Probabilities (2003). Earthquake probabilities in the San Francisco Bay region: 2002-2031, Open File Report 03-214, U.S. Geological Survey, U.S. Department of the Interior, Denver, Colorado.

16. Youngs, R.R., Arabasz W.J., Anderson R.E., Ramelli A.R., Ake J.P., Slemmons D.B., McCalpin J.P., Doser D.I., Fridrich C.J., Swan III F.H., Rogers A.M., Yount J.C., Anderson L.W., Smith K.D., Bruhn R.L., Knuepfer P.L.K., Smith R.B., DePolo C.M., O'Leary D.W., Coppersmith K.J., Pezzopane S.K., Schwartz D.P., Whitney J.W., Olig S.S., Torro G.R. (2003). A methodology for probabilistic fault displacement hazard analysis (PFDHA), *Earthquake Spectra* **19:1**, 191-219.